Table II. Parameters Used in the Extended-Hückel Calculations

	orbital	H_{ii} (eV)	ζ_1 (C_1[a])	ζ_2 (C_2[a])
Rh	4d	−12.73	5.54 (0.5563)	2.40 (0.6119)
	5s	−9.01	2.135	
	5p	−4.53	2.099	
I	5s	−18.0	2.68	
	5p	−12.7	2.32	
Cl	3s	−30.0	2.033	
	3p	−15.0	2.033	
F	2s	−40.0	2.425	
	2p	−18.1	2.425	
H	1s	−13.6	1.3	
C	2s	−21.4	1.625	
	2p	−11.4	1.625	

[a] Coefficients in the double-ζ d orbital expansion.

or semi-infinite systems such as surfaces, interfaces, and defects.

Conclusions for the rhodium chains are the following: (1) The length of the central Rh–Rh bond can be tuned by adjusting the electronegativity of the end-capping ligands. Highly electronegative caps such as fluoride give a short bond; less electronegative capping ligands such as iodide give a longer bond and nearly equal Rh–Rh bond lengths along the chain. The effect can be described as a ligand-induced mixing of MO's from the uncapped oligomer or of crystal orbitals from the infinite polymer. (2) For longer chains and high d electron counts (all rhodiums d^7–d^8), the HOMO must have Rh z^2 character and appear at an energy within the z^2 band of the infinite polymer. The HOMO–LUMO gap will smoothly decrease with increasing chain length. (3) Preferred cluster electron counts can be found by looking for low densities of states in the corresponding infinite solid. For the known molecule $[Rh_4(CN(CH_2)_3NC)_8Cl]^{5+}$, and for longer oligomers, they appear within the steep z^2 band of the infinite polymer—at electron counts near d^7–d^8.

Acknowledgment. We are grateful to Boon Teo for the inspiration to attack this problem and to H. A. Scheraga, who provided the support for L.P.'s stay in the United States. In addition, R.W. thanks Susan A. Jansen for helpful discussions and moral support, Peter P. Edwards and John Boland for useful suggestions regarding possible applications, and the Cornell University Materials Science Center and the NSF for support (Grant DMR 87422702).

Appendix

All calculations were performed with orbital exponents and Coulomb integrals taken from previous work[60] and listed in Table II. Idealized polyene geometries had C–C bond lengths of 1.4 Å, C–H bond lengths of 1.1 Å, and all angles of 120°. Rhodium–rhodium distances of 2.85 Å were taken to approximate Rh–Rh single bonds.[61] Rhodium–hydrogen (1.65 Å), Rh–Cl (2.63 Å), and Rh–I (2.76 Å) bond lengths were taken from published crystal structures.[56,62] Rh–F bond distances were estimated from the Rh–Cl distance and covalent radii (qualitative conclusions are valid over a range of Rh–X bond lengths of at least 0.5 Å). Idealized Rh coordination geometries were used so that all bond angles were 90° or 180°.

(60) (a) Hoffmann, R.; Minot, C.; Gray, H. B. *J. Am. Chem. Soc.* **1984**, *106*, 2001. (b) Canadell, E.; Eisenstein, O. *Inorg. Chem.* **1983**, *22*, 2398. (c) Summerville, R. H.; Hoffmann, R. *J. Am. Chem. Soc.* **1976**, *98*, 7240. (d) Andersen, A. B.; Hoffmann, R. *J. Chem. Phys.* **1974**, *60*, 4271.
(61) Mann, K. R.; Bell, R. A.; Gray, H. B. *Inorg. Chem.* **1979**, *18*, 2671.
(62) Balch, A. L.; Olmstead, M. M. *J. Am. Chem. Soc.* **1979**, *101*, 3128.

Trans-Edge-Sharing Molybdenum Octahedra: A Reciprocal Space Approach to Metal–Metal Bonding in Finite Chains[1]

Ralph A. Wheeler*,† and Roald Hoffmann*

Contribution from the Department of Chemistry and Materials Science Center, Cornell University, Ithaca, New York 14853. *Received January 25, 1988*

Abstract: Metal–metal bond lengths alternate at the apices of trans-edge-sharing octahedra in $In_{11}Mo_{40}O_{62}$. The bond alternation is a consequence of finite chain length: it is absent in $NaMo_4O_6$, the analogous infinite chain with a similar electron count. We trace the observed distortion to a set of σ levels with x^2–y^2 character and a nodal structure similar to the π levels of hydrocarbon polyenes. The apical pairing distortion mixes these levels with orbitals on basal molybdenums and enhances metal–metal bonding perpendicular to the chain, especially at the ends of the molecules. A second distortion involving octahedral tilting is found equally favorable for chains with an odd number of octahedra and a new charge partitioning between the clusters of $In_{11}Mo_{40}O_{62}$ is suggested. A newly developed linear combination of crystal orbitals (LCCO) method aids in comparing orbitals of the finite and infinite chains.

Solid-state chemistry is a burgeoning field, with new compounds and concepts being discovered almost daily. Unusual structures beget novel properties; fascinating new behavior fuels the search for still more compounds. From the synergism between chemistry and physics, patterns are beginning to develop. An understanding of solid-state structures and properties is emerging.

One key, unifying concept for materials chemistry and physics is the question of dimensionality. Extended, three-dimensional structures are often discussed in terms of smaller units such as layers,[2] chains,[3] or clusters,[4] but one may question the validity of such a picture. Are the fragments that make up the solid weakly coupled, or is the compound actually three-dimensional? A chemical approach to this puzzle involves searching for chemical

† Current address: Department of Chemistry, University of Houston; Houston, TX 77204-5641.

(1) Based on: Wheeler, R. A. Ph.D. Thesis, Cornell University, October, 1987; Chapter III.

(2) (a) O'Keeffe, M.; Hyde, B. G. *Philos. Mag.* **1980**, *295A*, 38. (b) Hulliger, F. *Structural Chemistry of Layer-Type Phases*; D. Reidel: Dordrecht, 1976. (c) Pearson, W. B. *The Crystal Chemistry and Physics of Metals and Alloys*; Wiley-Interscience: New York, 1972.

(3) (a) *Crystal Chemistry and Properties of Materials with Quasi-One-Dimensional Structures*; Rouxel, J., Ed.; D Reidel: Dordrecht, 1986. (b) *Electronic Properties of Inorganic Quasi-One-Dimensional Compounds*; Monceau, P., Ed.; D. Reidel: Dordrecht, 1985; Vol. I–II. (c) *Extended Linear Chain Compounds*; Miller, J. S., Ed.; Plenum: New York, 1982; Vol. 1–3. (d) *Highly Conducting One-Dimensional Solids*; Devreese, J. T., Evrard, R. P., Van Doren, V. E., Eds.; Plenum: New York, 1979.

0002-7863/88/1510-7315$01.50/0

bonds—especially molecules and clusters—in new solid-state compounds. Relevant questions concern cluster size and the strength of the coupling between clusters. How weak, for example, must the coupling be before the solid loses its three-dimensional character? How does cluster size affect the interaction between molecules and ultimately determine a compound's physical properties? Such questions as these are fundamental and lie at the heart of modern solid-state chemistry.

In this contribution, we analyze the metal–metal bonding in molybdate clusters made up of four and five trans-edge-sharing octahedra. The preferred distortion from chains of equidistant molybdenums will depend on the number of octahedra in the chain.

Finite and Infinite Chains of Octahedra

Although seeing clusters in solids is a persistent theme in solid-state chemistry,[4] making clusters where only extended structures exist is a significant and exciting experimental challenge. The Chevrel phases are one area where the challenge has been met, as the infinite Mo_6X_6 chain, as well as finite chains containing up to nine face-sharing octahedra are known.[4g] The group led by Arndt Simon has provided several, more recent examples of clusters literally cut from the solid. $Mo_{18}O_{28}^{7-}$ (**2**) and $Mo_{22}O_{34}^{8-}$ (**3**)[5] occur in $In_{11}Mo_{40}O_{62}$ and are derived from the $Mo_4O_6^-$ infinite

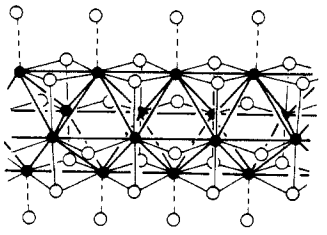

1

$^1_\infty[Mo_4O_6^-]$

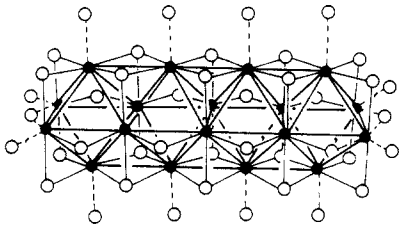

2

$Mo_{18}O_{28}^{7-}$

chain (**1**)[6] by introducing structural disorder at regular intervals along the chain.

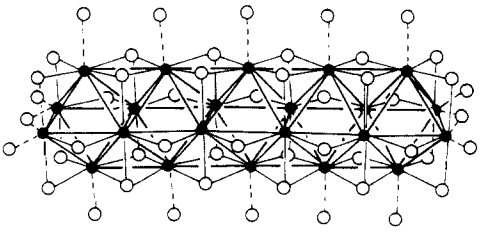

3

$Mo_{22}O_{34}^{8-}$

The molybdenum oxides, **1**–**3**, are part of a much larger story of reduced metal halides and chalcogenides with structures based on octahedral M_6 clusters.[7,4a,4d-f] One common example, the M_6X_{12} cluster that forms the basic building block of $NaMo_4O_6$ and $In_{11}Mo_{40}O_{62}$, is shown in **4**.

$\{[M_6X_{12}]X_6\}^{4-}$

M = Nb, Ta

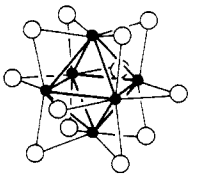

4

The Mo_6X_{12} unit consists of an octahedron of six molybdenum atoms, with each edge of the octahedron bridged by a ligand X. An alternative, idealized view of this 6–12 cluster has the X ligands in the middle of each edge of a cube, with a Mo atom at the center of each face (**5**). In the idealized geometry, each molybdenum would have a square-planar coordination environment. Since the molybdenums of **4** are sunken into the faces of the cube, instead

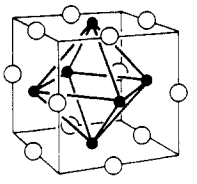

5

of having square-planar D_{4h} local symmetry each Mo resembles an inorganic C_{4v} ML_4 fragment. Six–twelve clusters of this type are common for X = halide,[8] but they are as yet unknown for X = O.[9]

The 6–12 clusters in **4** can be fused by sharing trans edges to give a variety of intriguing compounds. The gadolinium halides[10]—$Gd_{10}Cl_{18}(C_2)_2$, $Gd_{10}Cl_{17}(C_2)_2$, and $Gd_{10}I_{16}(C_2)_2$—are the smallest possible chains of edge-sharing octahedra. They are formed by fusing just two octahedral fragments to give the structure shown in **6**. The Gd octahedra in **6** share a common edge, while the other edges remain bridged by halide ligands. The C_2 units in the Gd clusters reside at the centers of the octahedra.

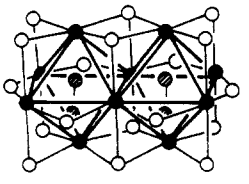

6

$Gd_{10}Cl_{18}(C_2)_2$

Continuing a chain of edge-sharing octahedra indefinitely gives the infinite chain compounds such as MMo_4O_6 (M = Na, In). A chain taken from the structure of $NaMo_4O_6$ is shown in **1** and has the same metal and ligand framework as the discrete 6–12 cluster, **4**. Like the metal atoms in the discrete 6–12 clusters, Mo atoms in the basal planes of the octahedra in $NaMo_4O_6$ approximate C_{4v} ML_4 fragments. In contrast, apical Mo atoms are

(4) (a) Simon, A. *Angew. Chem.* **1981**, *93*, 1. *Angew. Chem., Int. Ed. Engl.* **1981**, *20*, 1. (b) von Schnering, H.-G. *Angew. Chem.* **1981**, *93*, 44. *Angew. Chem., Int. Ed. Engl.* **1981**, *20*, 33. (c) Corbett, J. D., Ed. Proceedings of the Symposium on Metal–Metal Bonding in Solid State Clusters and Extended Arrays. In *J. Solid State Chem.* **1985**, *57*, No. 1. (d) Corbett, J. D.; McCarley, R. E., in ref 3a, p 179. (e) McCarley, R. E. *Philos. Trans. R. Soc. (London)* **1982**, *308A*, 141. (f) Corbett, J. D. *Acc. Chem. Res.* **1981**, *14*, 239. (g) Chevrel, R.; Sergent, M. in ref 3a, p 315. (h) Schäfer, H.; von Schnering, H.-G. *Angew. Chem.* **1964**, *76*, 832.

(5) (a) Simon, A.; Mertin, W.; Mattausch, Hj.; Gruehn, R. *Angew. Chem.* **1986**, *98*, 831. *Angew. Chem., Int. Ed. Engl.* **1986**, *25*, 845. (b) Mattausch, Hj.; Simon, A.; Peters, E.-M. *Inorg. Chem.* **1986**, *25*, 3428. (c) Simon, A.; Mattausch, Hj.; Peters, E.-M. *Z. Kristallogr.* **1986**, *174*, 188.

(6) Torardi, C. C.; McCarley, R. E. *J. Am. Chem. Soc.* **1979**, *101*, 3963.

(7) Corbett, J. D. *J. Solid State Chem.* **1981**, *37*, 335.

(8) (a) Vaughan, P. A.; Sturtevant, J. H.; Pauling, L. *J. Am. Chem. Soc.* **1950**, *72*, 5477. (b) Koknat, F. W.; McCarley, R. E. *Inorg. Chem.* **1974**, *13*, 295. (c) Simon, A.; von Schnering, H.-G.; Wöhrle, H.; Schäfer, H. *Z. Anorg. Allg. Chem.* **1965**, *339*, 155. (d) Bauer, D.; von Schnering, H.-G.; Schäfer, H. *J. Less-Common Met.* **1965**, *8*, 388. (e) Schäfer, H.; von Schnering, H.-G.; Niehus, K.-J.; Nieder-Vahrenholz, H. G. *J. Less-Common Met.* **1965**, *9*, 95. (f) Bauer, D.; von Schnering, H.-G. *Z. Anorg. Allg. Chem.* **1968**, *361*, 259.

(9) The only presently known oxide clusters with isolated M_6 octahedra are $Mg_3Nb_6O_{11}$ and $Mn_3Nb_6O_{11}$: (a) Marinder, B. O. *Chem. Scr.* **1977**, *11*, 97. (b) Abbattista, F.; Rolando, P. *Ann. Chim. (Rome)* **1971**, *61*, 196.

(10) (a) Simon, A.; Warkentin, E.; Masse, R. *Angew. Chem.* **1981**, *93*, 1071. *Angew. Chem., Int. Ed. Engl.* **1981**, *20*, 1013. (b) Warkentin, E.; Masse, R.; Simon, A. *Z. Anorg. Allg. Chem.* **1982**, *491*, 323. (c) Simon, A.; Warkentin, E., in press.

bonded to oxygens on adjacent chains to give them square-pyramidal coordination environments. All Mo–O distances in $NaMo_4O_6$ are in the range 2.014–2.067 Å. The metal–metal bonded chains of trans-edge-sharing octahedra are thus linked in a three-dimensional array by sharing oxygens with neighboring clusters.

Metal–metal bonded chains such as those found in $NaMo_4O_6$ can be fused to give a still richer variety of compounds. Several examples are mentioned here: the double chains found in Er_7I_{10},[11] Sc_7Cl_{10},[12] Tb_6Br_7, and Er_6I_7;[13] the double layer compounds such as ScCl,[14] YCl,[15] LaBr, and other rare earth halides;[16] or the truly three-dimensional extreme of condensed M_6 units, NbO[17] and TiO.[18] A number of these compounds have been the subject of theoretical studies. They show varying degrees of M–M bonding depending on factors such as M–M distances and electron counts.[19–21] The current study will focus on metal–metal bonding in the finite chain compounds $Mo_{18}O_{28}^{7-}$ and $Mo_{22}O_{34}^{8-}$ and their connection to the infinite $Mo_4O_6^-$ chain.

The cluster compounds found in $In_{11}Mo_{40}O_{62}$ and shown in **2** and **3** are related to $NaMo_4O_6$ in an obvious way: they are finite chain analogues of the $Mo_4O_6^-$ infinite chain. **2** is a chain of four edge-sharing Mo octahedra; **3** contains five such octahedra. Like the infinite chain, the cluster compounds $Mo_{18}O_{28}^{7-}$ and $Mo_{22}O_{34}^{8-}$ are linked to neighboring chains by sharing their oxygen atoms with apical molybdenums on another cluster. The clusters are also linked together by sharing oxygen atoms at the ends of the chain.

The formal d electron count for the three compounds is arrived at by assigning each oxide ligand a 2– formal charge. For $Mo_4O_6^-$, eleven positive charges are required on the Mo to balance the six negatively charged oxygens. Since molybdenum is a d^6 transition metal, the four molybdenums have 24 – 11 = 13 d electrons. Although short In–In contacts in $In_{11}Mo_{40}O_{62}$ make the cluster electron counts for **2** and **3** slightly ambiguous, assigning two electrons to each In–In bond and the remaining In electrons to the Mo clusters allows one to formulate the compound as $(In_5)^{7+}(In_6)^{8+}Mo_{40}O_{62}^{15-}$. We will argue later that this charge partitioning agrees qualitatively with calculations on the separate molybdate/In subsystems. A further partitioning of the 15 minus charges among the Mo clusters, based on summing Mo–O bond orders,[5b] gives $Mo_{18}O_{28}^{7-}$ (**2**) and $Mo_{22}O_{34}^{8-}$ (**3**). This charge partitioning between the two clusters will merit comment later. The assigned 7– charge and a 2– formal charge on the oxide ligands gives $Mo_{18}O_{28}^{7-}$ a d electron count of 108 – 49 = 59. For 18 molybdenums, this electron count is equivalent to approximately 13.1 electrons per "Mo_4" unit. Similarly, $Mo_{22}O_{34}^{8-}$ has 132 – 60 = 72 d electrons, or 13.1 electrons per "Mo_4".

Although the three compounds $Mo_4O_6^-$, $Mo_{18}O_{28}^{7-}$, and $Mo_{22}O_{34}^{8-}$ have similar structures and electron counts, metal–metal bonding within the clusters shows significant differences from Mo–Mo bonding in the infinite chain compound, $Mo_4O_6^-$. **7** shows the metal framework of $Mo_4O_6^-$, along with some relevant Mo–Mo distances. Molybdenum atoms located at the apices of the octahedra are uniformly spaced by 2.86 Å along the chain. Molybdenums located along the basal planes of the octahedra are also separated by the same distance, 2.86 Å, everywhere in the chain. The Mo–Mo distances in $Mo_4O_6^-$ can be contrasted with

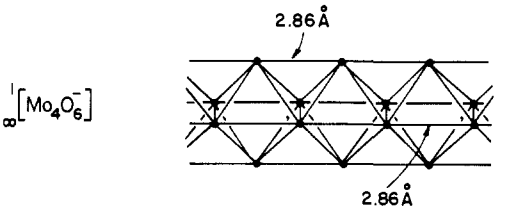

7

those in $Mo_{18}O_{28}^{7-}$ and $Mo_{22}O_{34}^{8-}$, whose metal frameworks are illustrated in **8** and **9**. **8** shows the strong bond alternation between apical Mo atoms of $Mo_{18}O_{28}^{7-}$ reminiscent of the C–C bond alternation in butadiene. The two outer Mo–Mo bonds are a short 2.66 Å, whereas the interior Mo atoms are separated by a much

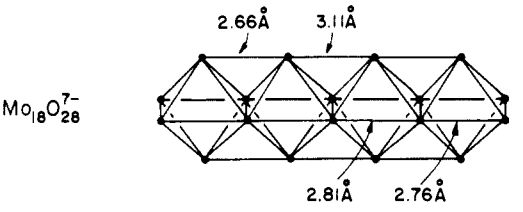

8

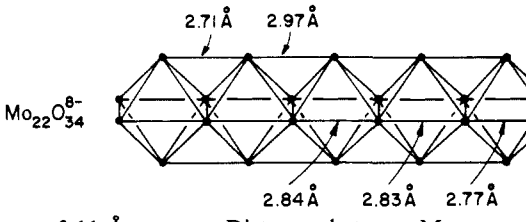

9

longer 3.11 Å contact. Distances between Mo atoms located in the basal planes of the octahedra show a similar bond alternation along the chain axis. End molybdenums are separated by 2.76 Å and the inner pair is separated by 2.81 Å. Although they are not shown in **8**, bond lengths between Mo atoms in the shared edges of the octahedra show an unusual short–long–short pattern, moving from the ends to the middle of the molecule.

Mo–Mo distances in $Mo_{22}O_{34}^{8-}$, **9**, show a long–short pattern similar to that just described for $Mo_{18}O_{28}^{7-}$. Apical Mo–Mo distances vary from one end of the molecule to the other as C–C distances in pentadienyl anion do: short (2.71 Å)–long (2.97 Å)–long (2.97 Å)–short (2.71 Å). As in $Mo_{18}O_{28}^{7-}$, Mo–Mo distances within the basal planes of the octahedra are shortest (2.77 Å) near the ends of $Mo_{22}O_{34}^{8-}$, longer (2.83 Å) between the center and ends, and longer still (2.78 Å) in the middle of the molecule. Perpendicular to the chain axis, bonds between basal molybdenums are shortest near the middle of the chain, longest between the middle and ends, and short again at the ends.

Mo–Mo bond lengths in the two clusters can be contrasted with those in $NaMo_4O_6$ and with Mo–Mo bonds in the quaternary extended solids such as $Sc_{3/4}Zn_{5/4}Mo_4O_7$ and $Ti_{1/2}Zn_{3/2}Mo_4O_7$.[22] The metal framework for one chain of the quaternary compounds is shown in **10**. Instead of simply pairing apical molybdenums, the entire metal octahedra in **10** tilt to give alternating bond

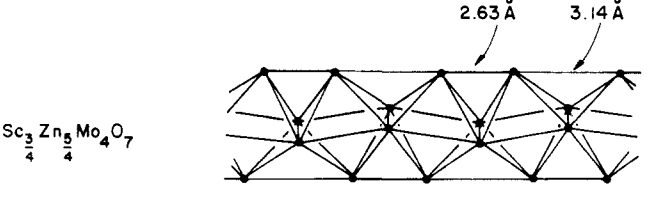

10

lengths along the infinite chain. These quaternary compounds are not the focus of the present study; they do, however, suggest

(11) Berroth, K.; Simon, A. *J. Less-Common Met.* **1980**, *76*, 41.
(12) Poeppelmeier, K. R.; Corbett, J. D. *Inorg. Chem.* **1977**, *16*, 1107.
(13) Berroth, K.; Mattausch, Hj.; Simon, A. *Z. Naturforsch.* **1980**, *B35*, 626.
(14) Poeppelmeier, K.; Corbett, J. D. *Inorg. Chem.* **1977**, *16*, 294.
(15) Mattausch, Hj.; Hendricks, J. B.; Eger, R.; Corbett, J. D.; Simon, A. *Inorg. Chem.* **1980**, *19*, 2128.
(16) (a) Simon, A.; Mattausch, Hj.; Holzer, N. *Angew. Chem.* **1976**, *88*, 685. *Angew. Chem., Int. Ed. Engl.* **1976**, *15*, 624. (b) Mattausch, Hj.; Simon, A.; Holzer, N.; Eger, R. *Z. Anorg. Allg. Chem.* **1980**, *466*, 7.
(17) Anderson, G.; Magneli, A. *Acta Chem. Scand.* **1957**, *11*, 1065.
(18) Watanabe, D.; Castles, J. R.; Jostous, A.; Matin, A. S. *Acta Crystallogr.* **1967**, *23*, 307.
(19) (a) Bullett, D. W. *Inorg. Chem.* **1980**, *19*, 1780. (b) Bullett, D. W. *Inorg. Chem.* **1985**, *24*, 3319.
(20) Satpathy, S.; Andersen, O. K. *Inorg. Chem.* **1985**, *24*, 2604.
(21) (a) Hughbanks, T.; Hoffmann, R. *J. Am. Chem. Soc.* **1983**, *105*, 3528. (b) Burdett, J. K.; Hughbanks, T. *J. Am. Chem. Soc.* **1984**, *106*, 3101.
(22) (a) McCarley, R. E. In *Inorganic Chemistry: Toward the Twenty-First Century*; Chisholm, M. H., Ed.; American Chemical Society: Washington, DC, 1983; ACS Symp. Ser. No. 211, p 273. (b) McCarley, R. E. *Polyhedron* **1986**, *5*, 51.
(23) (a) Hoffmann, R.; Lipscomb, W. N. *J. Chem. Phys.* **1962**, *36*, 2179. (b) Hoffmann, R. *J. Chem. Phys.* **1963**, *39*, 1397.

an alternative way to form bonds between apical molybdenums in the cluster compounds considered below.

In this paper we present first a discussion of $Mo_{18}O_{28}^{7-}$ that is based on extended-Hückel calculations[23] for idealized structures with equal Mo–Mo bond lengths. The distortion mode that forms short or long apical Mo–Mo bonds depends strongly on electron count and on the number of octahedra in the chain. Specific electron counts are suggested for even- and odd-member chains where either a simple pairing of apical molybdenums or a tilting of the Mo octahedra should be preferred. Results for the known four- and five-member chains are extrapolated to larger clusters and the results contrasted with Mo–Mo bonding in the infinite $Mo_4O_6^-$ chain. The comparison between the infinite and the large, finite chains is aided by a linear combination of crystal orbitals (LCCO) approach recently described.[24] The method expresses cluster MO's in terms of crystal orbitals of the solid and is used here to compare $Mo_{18}O_{28}^{7-}$ and $Mo_{22}O_{34}^{8-}$ directly with $Mo_4Mo_6^-$. The influence of apical Mo–Mo pairing on bonds between basal Mo atoms at the ends of the molecule is noted. Finally, a repartitioning of the electrons between the two clusters found in $In_{11}Mo_{40}O_{62}$ is suggested.

The MO's of Idealized $Mo_{18}O_{28}^{7-}$

Mo–Mo bonding in $Mo_{18}O_{28}^{7-}$ can be built up from the orbitals of its component ML_4 and ML_5 fragments, shown darkened in **11**. The apical Mo atoms, with their square pyramidal coordination, correspond to inorganic ML_5 fragments, whereas the basal Mo atoms are C_{2v} ML_4 fragments. The corresponding orbitals are displayed in **12**. They are well-known[25] and can be derived from the octahedral t_{2g} and e_g sets. In the octahedron, the e_g orbitals have metal–ligand σ^* character and are composed of the

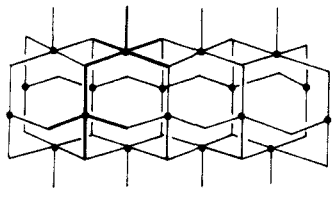

11

z^2 and xy orbitals for the coordinate system drawn in **12**. The t_{2g} set is nonbonding. When ligands are removed to give either

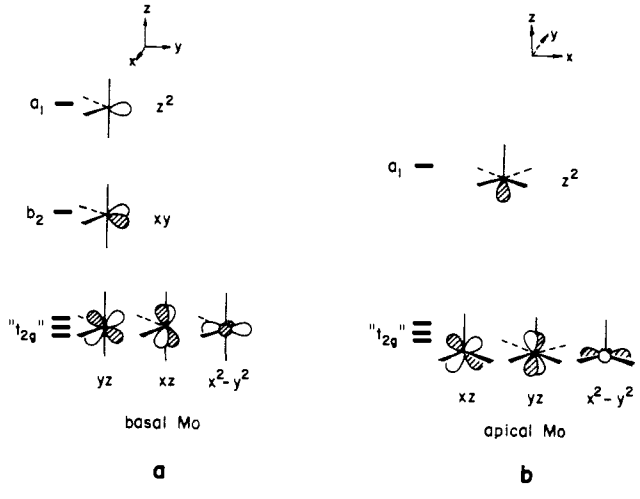

12

the ML_4 or ML_5 fragments, the t_{2g} set is unaffected. The e_g orbitals, on the other hand, will split into an a_1 and a lower energy b_2 level when two ligands are removed to give the ML_4 unit. The a_1 consists mainly of metal z^2 and the b_2 orbital has primarily metal xy character, as shown in **12a**. A similar energy lowering of z^2 when one ligand is removed from the octahedron gives the orbital splitting for ML_5 shown in **12b**. The xy level remains strongly σ antibonding and is not drawn in **12b**. Mo–Mo bonding will arise mainly from orbital interactions within the nonbonding t_{2g} levels, particularly since the x^2-y^2 orbitals are oriented to give a strong σ overlap between apical and between basal molybdenum atoms.

Turning on the metal–metal interactions will broaden the discrete levels into "bands", shown schematically in **13**. The e_g orbitals start out high in energy and are oriented incorrectly for good metal–metal overlap, so they contribute little to metal–metal

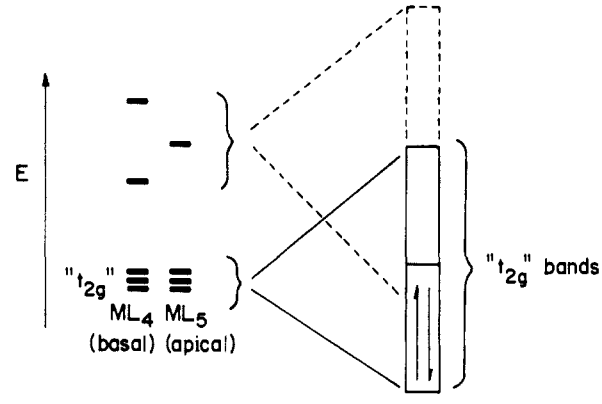

13

bonding. The t_{2g} set begins at low energy and one member, the x^2-y^2 orbital on both the ML_4 and ML_5 fragments, is oriented for good σ overlap with the orbitals on neighboring metal atoms. Thus the bottom of the metal d block should be composed of t_{2g} levels with metal–metal bonding character. Among the t_{2g} orbitals, the lowest energy levels should have x^2-y^2 character since x^2-y^2 has the greatest dispersion. The result is strong Mo–Mo bonding even at relatively low d electron counts.

Figure 1 displays the calculated ordering of Mo x^2-y^2 levels for an idealized model $Mo_{18}O_{28}^{7-}$ structure with all Mo–Mo distances equal to 2.8 Å. The model, shown in **14**, has H atoms placed at a bonding distance from edge-bridging oxygens to simulate the effect of Mo atoms in neighboring clusters. Terminal oxygens on the apical molybdenums are replaced with model "H" ligands designed to reproduce the crystal field splitting of a σ-bonded oxygen atom.[21a]

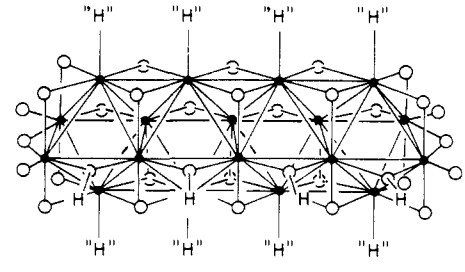

14

Orbitals with mainly Mo x^2-y^2 character are drawn out in Figure 1 and their symmetries are given in the point group D_{2h}. Orbitals with other AO compositions are omitted from the figure. The orbitals drawn in Figure 1 are easily understood by considering the x^2-y^2 orbitals concentrated on apical and on basal molybdenums separately and by recognizing their resemblance to polyene π levels. The apical molybdenums form a four-atom chain, whereas basal Mo_2 units make a five-membered chain. Of course, the apical–basal separation is not exact and several interesting consequences will result from the interaction between orbitals on apical and basal molybdenums.

The lowest energy orbital drawn in Figure 1, labeled $1a_g$, is the combination of basal molybdenum x^2-y^2 that is bonding between Mo_2 units and completely bonding along the chain. $1b_{3u}$ and $5a_g$ are singly and doubly noded chain orbitals, respectively, with

(24) (a) Wheeler, R. A. Ph.D. Thesis, Cornell University, October, 1987; Chapter II. (b) Wheeler, R. A.; Piela, L.; Hoffmann, R. *J. Am. Chem. Soc.*, preceding paper in this issue.

(25) (a) Elian, M.; Hoffmann, R. *Inorg. Chem.* **1975**, *14*, 1058. (b) Albright, T. A.; Burdett, J. K.; Whangbo, M.-H. *Orbital Interactions in Chemistry*; Wiley-Interscience: New York, 1985.

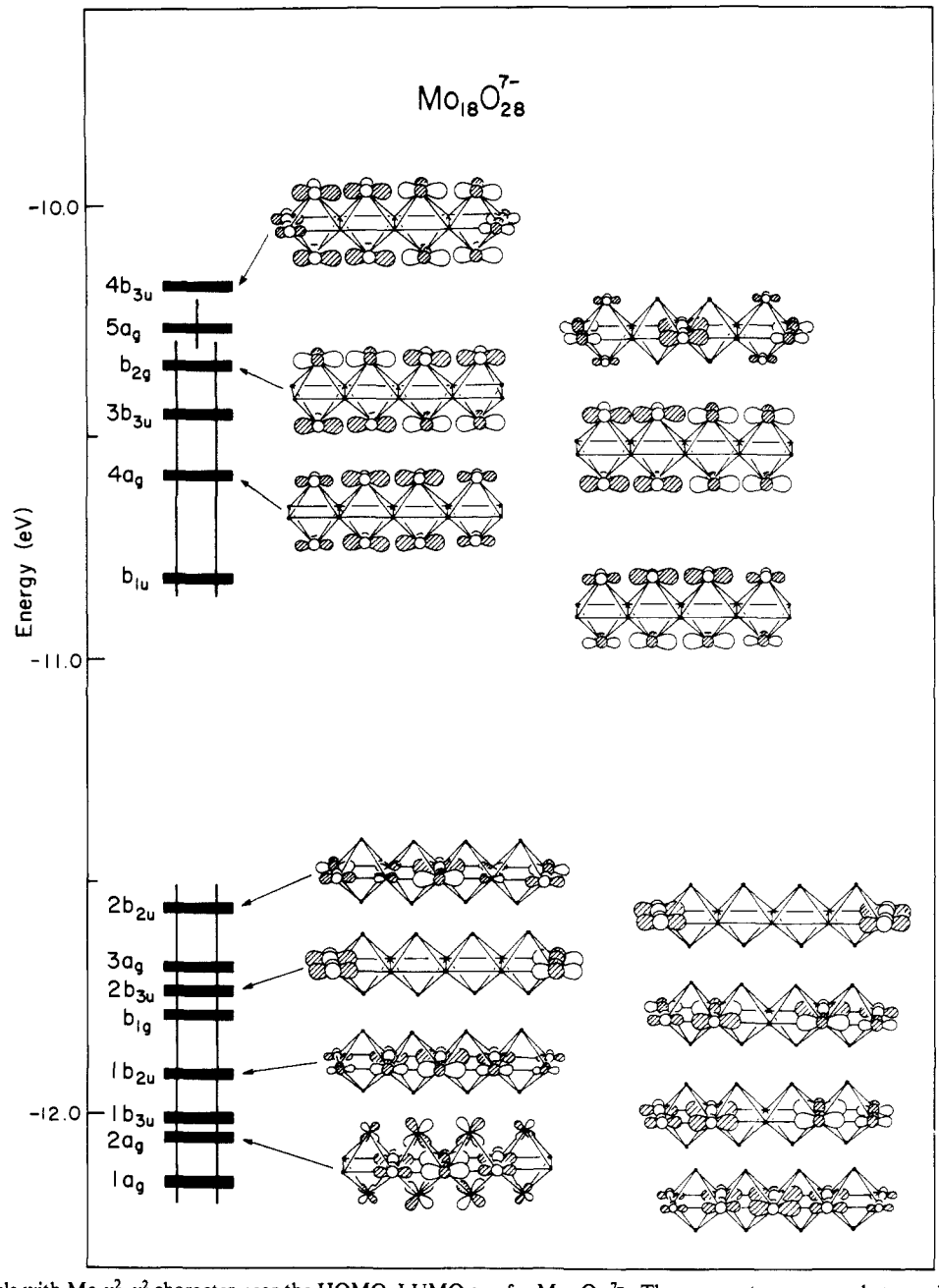

Figure 1. Energy levels with Mo x^2-y^2 character near the HOMO–LUMO gap for $Mo_{18}O_{28}^{7-}$. The apparent energy gap between b_{1u} and $2b_{2u}$ is actually filled by six levels of various AO compositions. Additional levels are also interspersed between the ten lower levels shown—$4a_g$ to $1a_g$.

bonding character within Mo_2 dimers. Likewise, the completely bonding ($1b_{2u}$), singly noded ($1b_{1g}$), and doubly noded ($2b_{2u}$) chain orbitals that are antibonding within the dimers appear at low energy. Because sets of three orbitals with similar nodal structure along the chain that are bonding *and* antibonding within Mo_2 fragments are occupied, their contributions to Mo–Mo bonding perpendicular to the chains approximately cancel. In reality, AO coefficients in the bonding levels are larger so that a small bonding interaction perpendicular to the chain is introduced by these six levels. An additional orbital with four nodal planes through apical molybdenums ($2a_g$), strongly bonding between molybdenums in the shared edges of the octahedra, also appears at low energy. This level is strongly stabilized by bonding interactions with apical molybdenums and contributes substantially to bonding within the central Mo_2 unit and within the Mo_2 fragments on either side of it. The end Mo_2 fragments are bonded by orbitals concentrated at the ends of the molecule, $2b_{3u}$ and $3a_g$. These orbitals have no obvious counterpart in polyene orbitals and will be discussed in more detail later.

x^2-y^2 orbitals on apical molybdenums can be understood in the same way as the orbitals concentrated on the basal Mo atoms. $1b_{1u}$ and $4a_g$ are completely bonding along the molecule's long axis and antisymmetric ($1b_{1u}$) or symmetric ($4a_g$) to the xy mirror plane. The corresponding singly noded orbitals, $3b_{3u}$ and $1b_{2g}$, also appear at low energy and are occupied. A third singly noded orbital, $4b_{3u}$, appears just above the LUMO for the symmetrical model compound with an electron count appropriate for $Mo_{18}O_{28}^{7-}$. This orbital also has a significant contribution from x^2-y^2 orbitals on basal molybdenums located at the molecule's ends. $4b_{3u}$ will become important later, but for now it is sufficient to note its bonding character between basal and apical Mo atoms.

The consequences of the orbital interactions described above are illustrated in **15**. **15** displays the Mo framework of $Mo_{18}O_{28}^{7-}$ along with overlap populations, a measure of bond order, for selected Mo–Mo bonds. For the apical molybdenum atoms the overlap populations mirror the experimental Mo–Mo bond lengths:

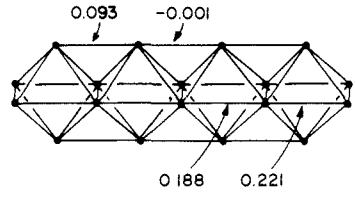

15

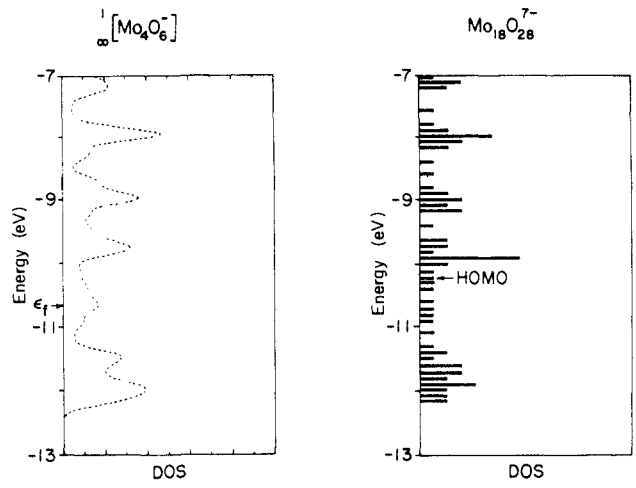

Figure 2. A comparison of the density of states for the infinite $Mo_4O_6^-$ chain (a, left) and the $Mo_{18}O_{28}^{7-}$ cluster (b, right). The cluster DOS shows all MO's in the energy range from −13 to −7 eV. No pronounced "band gap", only a low density of states, appears near the HOMO of $Mo_{18}O_{28}^{7-}$ (in the idealized structure with all apical Mo–Mo distances equal).

the larger overlap population (0.093) occurs where the short Mo–Mo bonds appear and a small, negative overlap population characterizes the molybdenums separated by the longer distance. We recall here the fact that the calculations are made with *equal* Mo–Mo bond lengths—thus the overlap population differentials are signs or hints of real bonding differences. Likewise, overlap populations between basal molybdenums along the chain axis follow the observed bond lengths, with larger overlap populations and shorter bonds near the ends of the molecule. Although they are not shown in **15**, overlap populations between molybdenums in the shared octahedral edges *do not* show the observed trend in bond lengths. Calculated overlap populations decrease from the center of the chain outward. Moving the apical molybdenums into their experimentally observed positions will be considered later, along with its effect on bonding between basal molybdenum atoms. But first, the comparison with the infinite $Mo_4O_6^-$ chain is made.

Molecular Orbitals as LCCO's

The crystal orbitals of the infinite $Mo_4O_6^-$ chain provide a second way to describe the orbitals of the $Mo_{18}O_{28}^{7-}$ cluster. The discussion of cluster MO's in terms of crystal orbitals of the extended solid complements the usual approach by allowing a direct assessment of cluster end effects, of the changes caused by cutting the cluster from the solid.

Parts a and b of Figure 2 compare the density of states (DOS) for the infinite $Mo_4O_6^-$ chain (Figure 2a) with the cluster density of states (Figure 2b). The two figures show a remarkably similar form, although several details are different. The double-peaked structure at −12 eV in the DOS of the infinite chain is reproduced for the cluster. Likewise, peaks in the densities of states appear in both plots near −9.75, −9, and −8 eV. The only obvious features in Figure 2b that are different from those in Figure 2a are the size of the peak near −10 eV and the absence of the small maximum near −10.5 eV. For the infinite chain, the Fermi energy—the energy of the highest occupied level—falls in the small peak near −10.5 eV; for the cluster, the HOMO is at higher energy but falls at a dip in the density of states.

The energy bands of $Mo_4O_6^-$ better expose the differences between the infinite chain and the finite cluster. Since the bands of $Mo_4O_6^-$ have been discussed by Hughbanks et al.,[21a] only the orbitals essential to metal–metal bonding in the finite chains will be considered here.

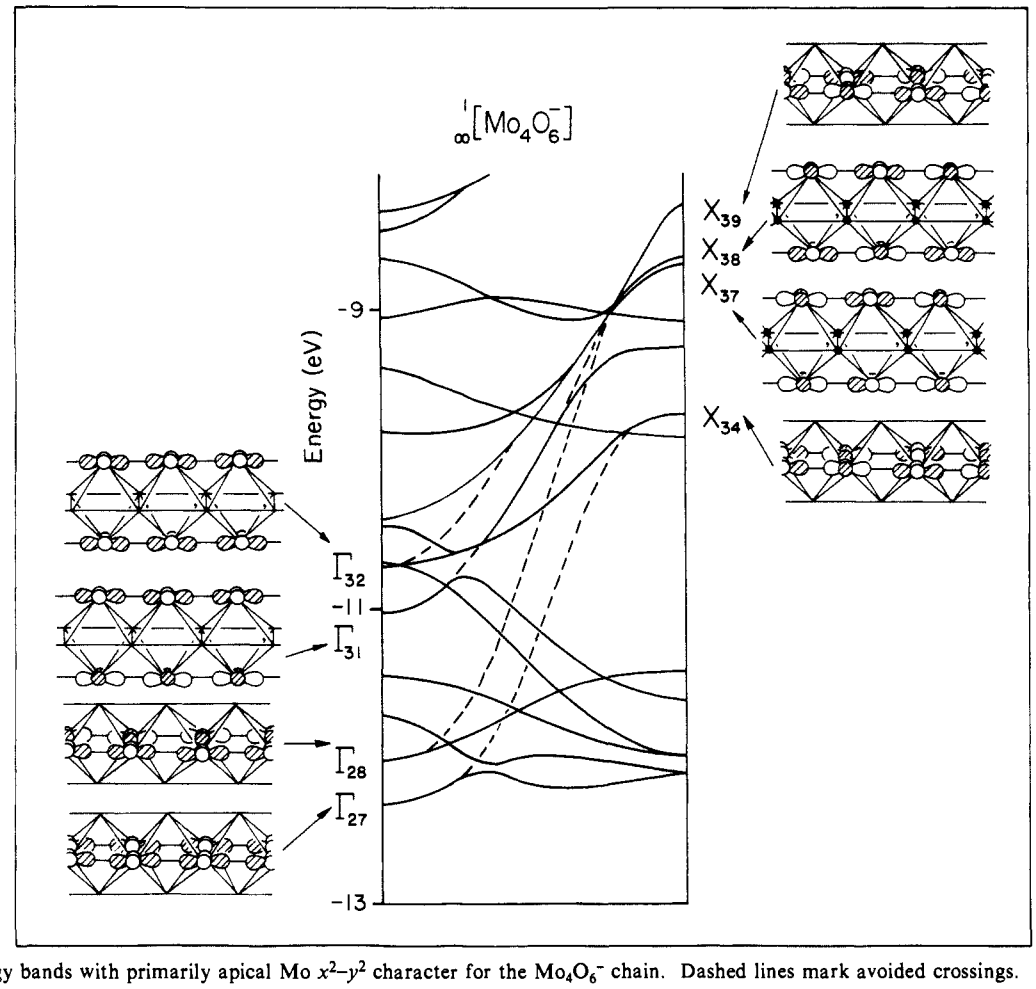

Figure 3. Energy bands with primarily apical Mo x^2-y^2 character for the $Mo_4O_6^-$ chain. Dashed lines mark avoided crossings.

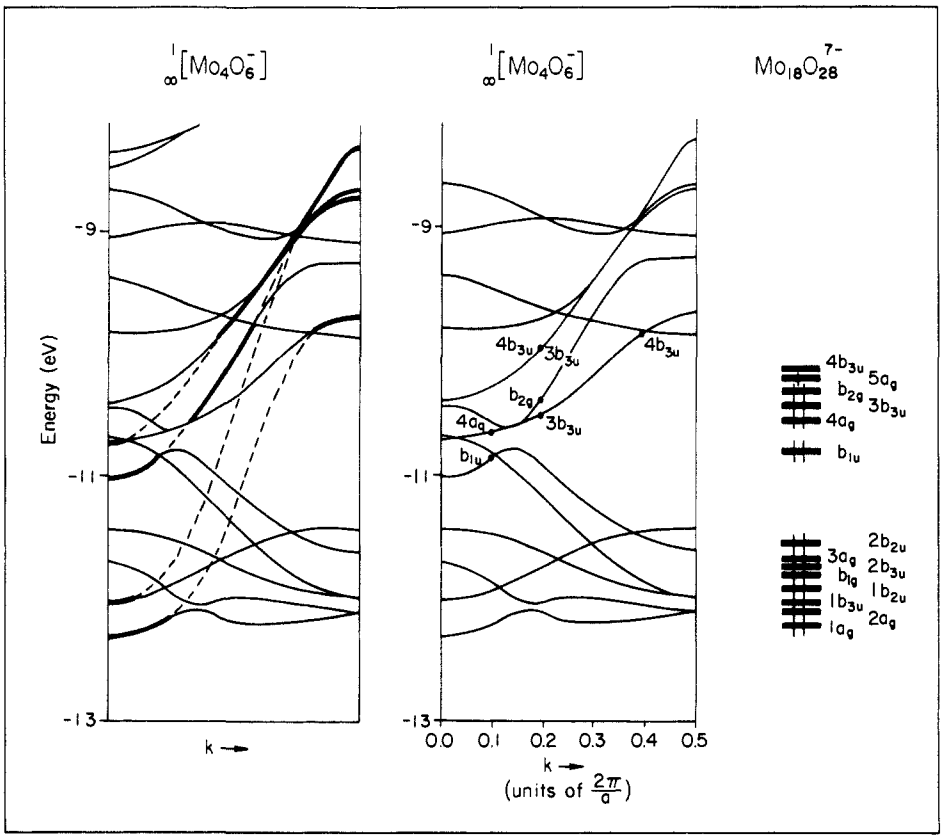

Figure 4. (a, left) Bands of the infinite chain, with avoided crossings marked by dashed lines. (b, middle) Bands of the $Mo_4O_6^-$ chain. k points chosen for the cluster MO calulation are marked at the bottom. Dots represent crystal orbitals making the dominant contribution to the cluster MO's whose symmetries are indicated. (c, right) MO's of the $Mo_{18}O_{28}^{7-}$ cluster having predominantly Mo x^2-y^2 character.

Bands near the Fermi energy of $Mo_4O_6^-$ are displayed in Figure 3. The bands composed of mainly metal x^2-y^2 are darkened and the orbitals corresponding to these bands at $k = 0$ and $k = \pi/a$ are labeled and drawn out in the figure. The lowest energy levels at $k = 0$, Γ_{27} and Γ_{28}, are concentrated on atoms in the basal planes to the octahedra and are completely bonding along the chain. Γ_{27} is symmetric to reflection in the xz plane and Γ_{28} is antisymmetric. Their counterparts at $k = \pi/a$ are completely antibonding along the chain and are labeled X_{34} and X_{39}. The dashed lines connecting the corresponding bands in Figure 3 show intended crossings and indicate the similar compositions of the levels at the point Γ ($k = 0$) and the point X ($k = \pi/a$). The actual avoided crossings between bands of the same symmetry mix the x^2-y^2 bands with other orbitals inside the Brillouin zone. As a result, the orbitals within the zone are not pure x^2-y^2 but have some mixed character depending upon which bands take part in the avoided crossing. This mixing inside the Brillouin zone will have important consequences later, when the crystal orbitals are mixed to form cluster MO's.

Crystal orbitals at $k = 0$ and concentrated on apical molybdenums (Γ_{31} and Γ_{32}) are the completely bonding combinations of apical x^2-y^2 orbitals. One is symmetric (Γ_{31}) and the other is antisymmetric (Γ_{32}) to the xy mirror plane. Like the basal orbitals, bands derived from Γ_{31} and Γ_{32} both undergo avoided crossings inside the Brillouin zone and correlate with their counterparts having antibonding character along the chain axis—X_{37} and X_{38}.

In recent work[24] a perturbation method was proposed for generating the orbitals of finite clusters or oligomers starting out from the simpler translationally delocalized crystal orbitals of an infinite extended solid or polymer. Operationally, the process goes as follows:

1. The band structure of the polymer (here $Mo_4O_6^-$) is computed.

2. The unit cell is enlarged (to an Mo_{16} unit in this example) and the bands are thus "folded back"[25b,26] to prepare for the perturbation of excising the cluster. A judicious choice of k points in the band calculation ensures that the crystal orbitals of the solid (actually approximate Wannier functions[24,27] for a large unit cell corresponding to the cluster) resemble the orbitals of the excised cluster as closely as possible.

3. A perturbation calculation introduces the capping atoms that complete the cluster, and which might have been missing in the "cutting out" of the cluster (here, the caps include two molybdenums and the oxygen necessary to make $Mo_{18}O_{28}^{7-}$).

In previous work,[24] the method was tested on polyenes and $(RhL_4)_n$ oligomers; the present study actually provides a much more stringent test of the method.

Figure 4 compares the band structure of $Mo_4O_6^-$ with the levels of $Mo_{18}O_{28}^{7-}$. Since the subsequent discussion will emphasize orbitals near the HOMO–LUMO gap for the cluster, only the bands concentrated on apical Mo x^2-y^2 atomic orbitals are highlighted by being darkened in Figure 4a. The same bands are reproduced in Figure 4b, along with hash marks indicating k points where orbitals from the band calculation were used to calculate cluster MO's. The symmetry labels in Figure 4b refer to the MO's whose dominant crystal orbital components are marked by the corresponding dots. For comparison, MO energy levels with primarily Mo x^2-y^2 character are indicated in Figure 4c.

Figure 4 highlights several interesting features of the LCCO method. First, the energy position and ordering of the crystal orbitals roughly parallels that of the analogous MO's. Dominant crystal orbitals appear near the bottom of the apical Mo x^2-y^2 band so that the metal–metal bonding nature of the MO's is reflected in the predominantly Mo–Mo bonding character of the

(26) (a) Gerstein, B. C. *J. Chem. Educ.* **1973**, *50*, 316. (b) Burdett, J. K. *Prog. Solid State Chem.* **1984**, *15*, 173. (c) Whangbo, M.-H. In *Crystal Chemistry and Properties of Materials with Quasi-One-Dimensional Structures*; Rouxel, J., Ed.; D. Reidel: Dordrecht, 1986; p 27.

(27) (a) Wannier, G. H. *Phys. Rev.* **1937**, *52*, 191. (b) Blount, E. I. In *Solid State Physics*; Seitz, F., Turnbull, D., Eds.; Academic: New York, 1962; Vol. 13, p 305.

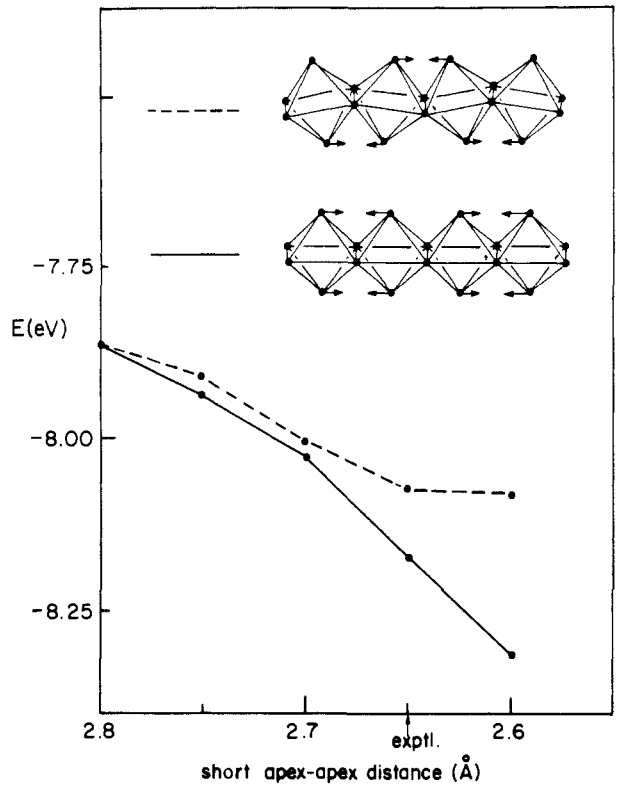

Figure 5. Changes in total energy for $Mo_{18}O_{28}^{7-}$ as apical molybdenums pair or octahedra tilt.

crystal orbitals. The energy ordering of the crystal orbitals marked in Figure 4b is also identical with the ordering of the corresponding MO's. Furthermore, most molecular orbitals correspond to one point on a Mo x^2-y^2 band corresponding to a crystal orbital at one of the chosen k points. This simply reflects the similar AO composition of the MO's and crystal orbitals and the fact that k points in the band calculation reflect the nodal structure of the molecular orbitals. Thus, b_{1u} and b_{2g} are derived from the apical Mo x^2-y^2 band that is antisymmetric to the xy reflection plane, and $4a_g$ is concentrated in the analogous band that is symmetric to reflection in the same plane. The $3b_{3u}$ level is largely composed of two crystal orbitals taken from the same k point. This is a result of the avoided crossing between the two bands and is a general feature of the LCCO scheme. Near an avoided crossing, a crystal orbital from each band will mix to give the correct cluster MO. The mixing serves to deconvolute the crystal orbitals and undo, to some extent, the effect of the avoided crossing. The result is cluster MO's derived from crystal orbitals with the correct AO composition, approximately correct nodal structure, and nearly the same energy as the final molecular orbitals.

The last level marked in Figure 4b, $4b_{3u}$, is an obvious exception to the mixing scheme just described: it is a combination of two crystal orbitals from different bands and different k points, with nearly equal weights. Although the two crystal orbitals originate from different bands, the parent bands have similar AO compositions due to an avoided crossing early in the Brillouin zone. **16** explicitly displays the combined apical and basal Mo x^2-y^2 nature of the crystal orbitals, as well as the character of the resulting cluster Mo, $4b_{3u}$. The basal x^2-y^2 character has cancelled everywhere in the $4b_{3u}$ level, except at the ends of the molecule. This cancellation is due to the nodal structure of the two combining crystal orbitals, which is set by their k values. The same effect is observed for other MO's, most notably the $2b_{3u}$ and $3a_g$ orbitals shown in **17**. $2b_{3u}$ and $3a_g$ are combinations of basal Mo x^2-y^2 orbitals, concentrated on terminal atoms of the chain, and symmetric or antisymmetric to reflection through the yz plane. The localization in the basal component of $4b_{3u}$ near the ends of the cluster will be important later, when the distortion involving the pairing of apical molybdenums is considered.

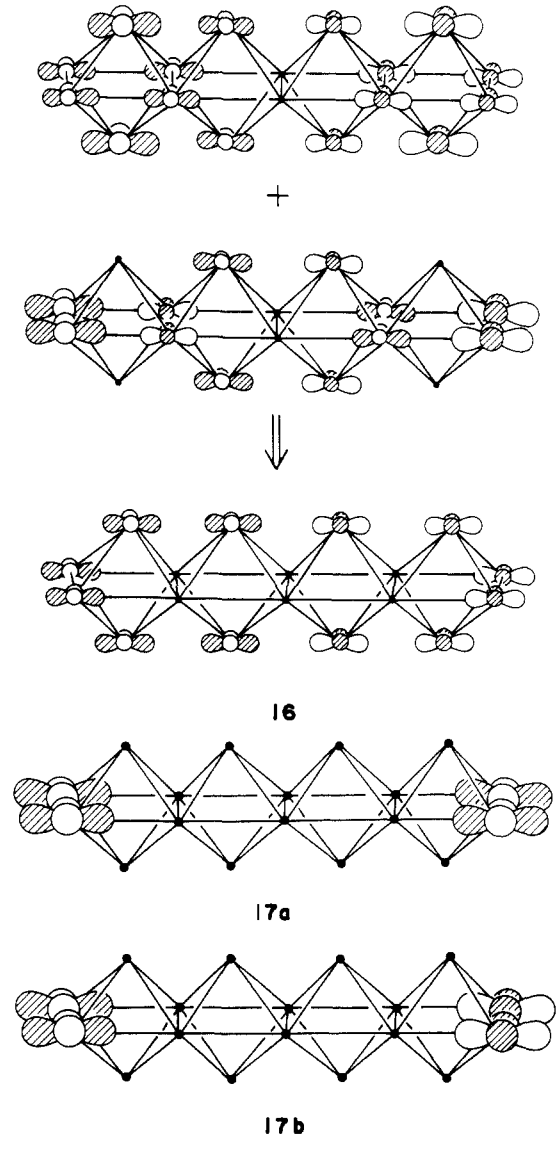

Distortions from the Idealized $Mo_{18}O_{28}^{7-}$

The energy changes for the idealized $Mo_{18}O_{28}^{7-}$ cluster are shown in Figure 5 for a pairing of apical molybdenums and for the octahedral tilting illustrated at the top of the figure. The energy drops in both cases but always remains lower for the pairing distortion. As the molybdenums approach closer than the observed 2.65-Å separation, the energy continues to decrease. This effect is a common artifact of the extended-Hückel method which tends to give equilibrium bond lengths that are too short. It arises in this case because the repulsive core of molybdenum d electrons is insufficient to counterbalance the increased Mo–Mo bonding as the atoms move together. The energy decrease upon distorting is, however, a valid indicator of the molecule's preference for the observed pattern of apical Mo–Mo distances.

A detailed examination of the individual levels of $Mo_{18}O_{28}^{7-}$ as the apical molybdenums pair up confirms that increased Mo–Mo bonding causes the energy lowering. Figure 6 is a correlation diagram showing the effect of the observed apical Mo–Mo bond alternation on selected MO's near the HOMO–LUMO gap of the $Mo_{18}O_{28}^{7-}$ cluster. Among x^2-y^2 orbitals concentrated on apical molybdenums, those that are completely bonding along the chain—$1b_{1u}$ and $4a_g$—drop slightly in energy. Overlap gained between end molybdenums is approximately compensated by that lost between the two central Mo atoms. Orbitals with a single node perpendicular to the chain axis are stabilized by an increased bonding interaction between outer molybdenums. The decreased antibonding overlap between central Mo orbitals enhances the energy lowering of these orbitals—primarily $3b_{3u}$ and $1b_{2g}$, but also $4b_{3u}$. For an electron count

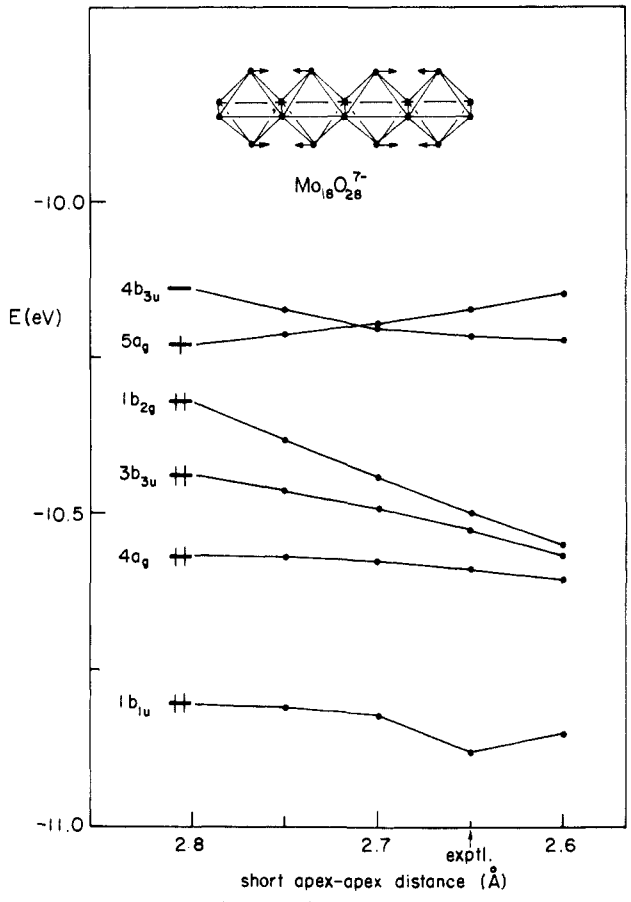

Figure 6. Correlation diagram showing the energy changes of levels concentrated on apical Mo x^2-y^2 and appearing near the HOMO–LUMO gap for $Mo_{18}O_{28}^{7-}$.

appropriate for $Mo_{18}O_{28}^{7-}$, the $4b_{3u}$ level drops below $5a_g$ and becomes singly occupied, but this may not be real. The energy gap that opens between the $1b_{2g}$ and $4b_{3u}$ levels and results for the $Mo_{22}O_{34}$ cluster to be presented later suggest that the Mo_{18} chain is better formulated as $Mo_{18}O_{28}^{6-}$ and that $4b_{3u}$ remains unoccupied.

Although $4b_{3u}$ is unoccupied when apical Mo atoms are paired, it nonetheless strengthens bonding between basal molybdenums at the ends of the cluster by mixing with $3b_{3u}$. The result is added basal Mo component at the ends of the molecule in the occupied $3b_{3u}$ level. This mixing of $4b_{3u}$ and $3b_{3u}$ boosts the overlap population between end Mo_2 pairs, but it is insufficient to make the pattern of overlap populations for the basal Mo_2 pairs agree with the observed bond lengths. It does, however, suggest an interesting analogy with surface chemistry. If the basal molybdenums at the ends of the chain represent the "surface" of the cluster, the mixing between $4b_{3u}$ and $3b_{3u}$ when apical molybdenums are paired suggests that surface reconstruction for the molybdate clusters (involving atom displacements parallel to the surface) is electronically coupled to surface relaxation (bond length changes perpendicular to the surface).[28]

The effect on orbital energies of the octahedral tilting distortion is displayed in Figure 7. As for the pairing distortion, the completely bonding $1b_{1u}$ and $4a_g$ levels, as well as the singly noded $3b_{3u}$, drop in energy. $1b_{2g}$, however, stays at constant energy as the more bonding interaction between end molybdenums is cancelled by the increased antibonding overlap between the central molybdenum pair. In addition, $1b_{2g}$ and $3b_{3u}$ have the same symmetry in the point group C_{2v}, after tilting, so they can mix. The effect of the mixing for the higher energy $1b_{2g}$ orbital is shown, exaggerated, in **18**. The constant energy of $1b_{2g}$ along the distortion coordinate is the reason that octahedral tilting is a higher

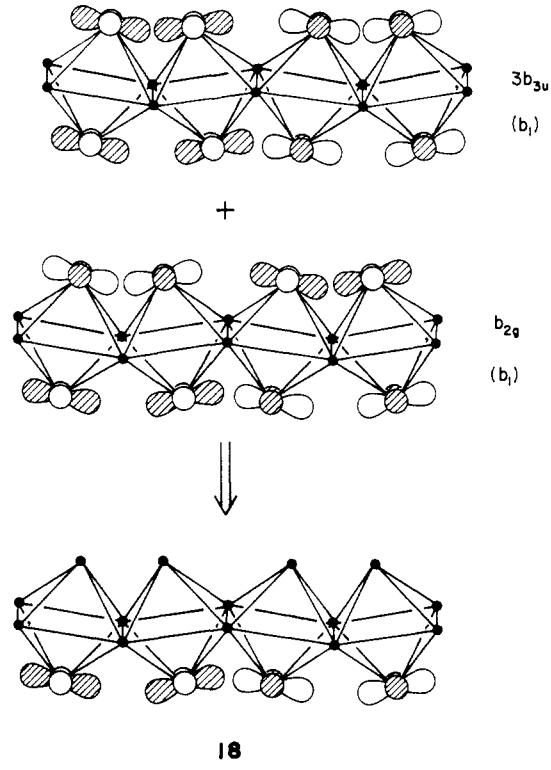

18

energy process than the pairing distortion. For the lower electron count appropriate for $Mo_{18}O_{28}^{4-}$, $1b_{2g}$ would be the empty LUMO and the energetics are reversed: octahedral tilting is favored over Mo pairing. Metal–metal bonding for the optimum electron counts favoring either Mo pairing or octahedral tilting is summarized in **19**. For $Mo_{18}O_{28}^{6-}$, $1b_{2g}$ is filled and pairing apical Mo atoms forms four strong Mo–Mo bonds; for lower electron counts, with $1b_{2g}$ empty, the favored octahedral tilting gives three metal–metal bonds between apical molybdenums. At higher electron counts, near where the quaternary molybdates show tilted octahedra, no

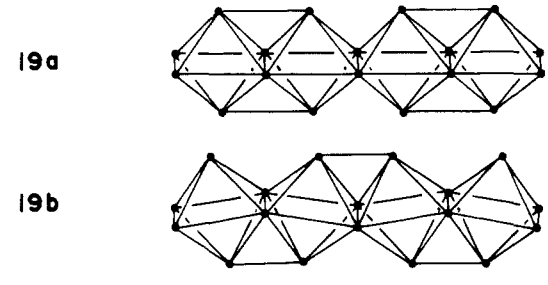

HOMO–LUMO gap opens for either distortion. It would be interesting, nonetheless, to characterize the $Mo_{18}O_{28}^{4-}$ cluster experimentally and to check the predicted distortion at lower electron counts.

The $Mo_{22}O_{34}^{8-}$ Cluster

Metal–metal bonding in the $Mo_{22}O_{34}^{8-}$ cluster can be understood in the same way as in $Mo_{18}O_{28}^{7-}$: low-energy x^2-y^2 levels on basal molybdenums, with apical Mo x^2-y^2 levels at the HOMO–LUMO gap. The completely bonding and singly noded basal levels give basal Mo pairing parallel to the chain axis, near the ends of the chain. Likewise, x^2-y^2 orbitals on apical molybdenums, displayed on the left of Figure 8, are filled through the singly noded levels. The lowest two levels in Figure 8 are completely bonding apical Mo x^2-y^2, and the next two each have one nodal plane perpendicular to the chain. The nodes for these levels, b_{2g} and $1b_{3u}$, pass through apical molybdenums on the

(28) The terms "surface relaxation" and "surface reconstruction" are sometimes used rather loosely, but relaxation refers here specifically to a change of interlayer spacing perpendicular to the surface: (a) Inglesfield, J. E. *Prog. Surf. Sci.* **1985**, *20*, 105. (b) Somorjai, G. A. *Chemistry in Two Dimensions: Surfaces*; Cornell University: Ithaca, 1981; p 127. (c) Estrup, P. J. In *Chemistry and Physics of Solid Surfaces*; Vanselow, R., Howe, R., Eds.; Springer-Verlag: Berlin, 1984; Vol. 5; p 205.

(29) Canadell, E.; Eisenstein, O.; Rubio, J. *Organometallics* **1984**, *3*, 759.

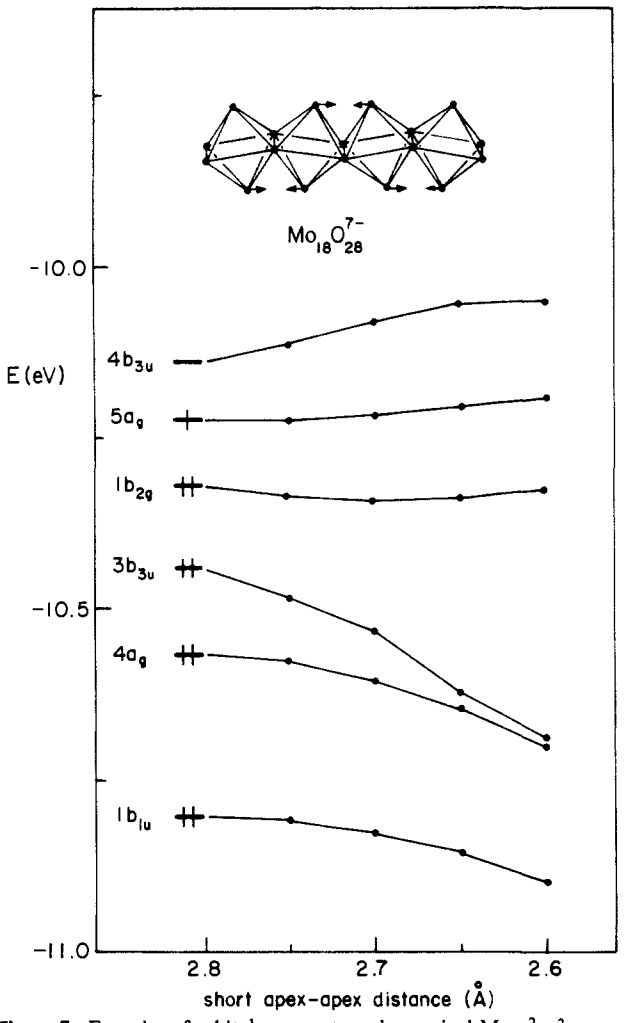

Figure 7. Energies of orbitals concentrated on apical Mo x^2-y^2 vary as octahedra tilt in $Mo_{18}O_{28}^{7-}$.

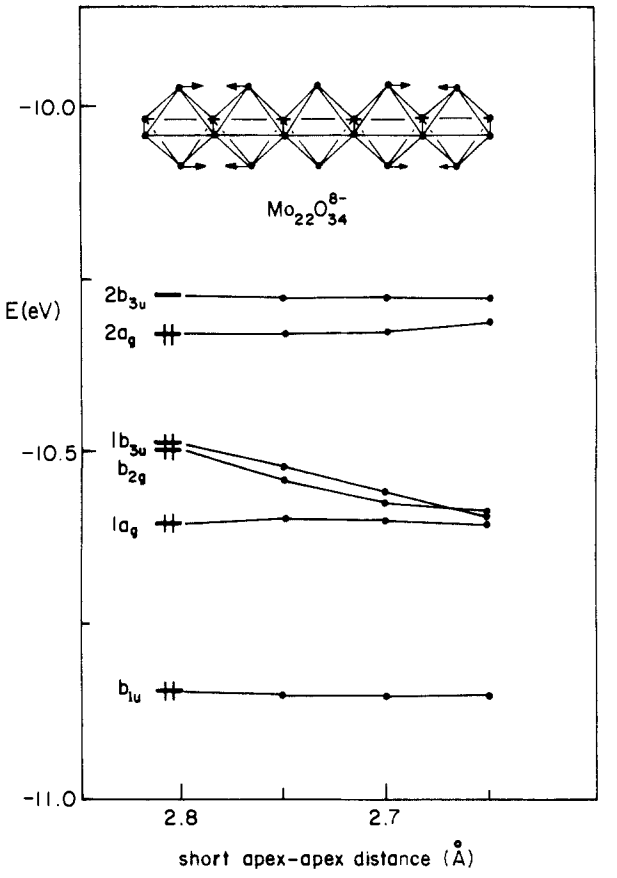

Figure 8. Pairing apical molybdenums in $Mo_{22}O_{34}^{8-}$ changes Mo x^2-y^2 orbital energies near the HOMO–LUMO gap. The second, apparent energy gap between $1a_g$ and b_{1u} is actually occupied by two levels not drawn in the figure.

central octahedron. $2a_g$ is included in the figure simply to mark the HOMO and does not contribute substantially to Mo–Mo bonding. $2b_{3u}$ has a similar composition to the $4b_{3u}$ level of $Mo_{18}O_{28}^{7-}$. $2b_{3u}$ is concentrated on apical Mo atoms and has one node perpendicular to the chain. It also has some small contribution from basal Mo x^2-y^2 at the ends of the cluster. The next level above $2b_{3u}$ is not shown in the figure; it appears near −10 eV, a full 0.5 eV above the LUMO for $Mo_{22}O_{34}^{8-}$.

Pairing apical molybdenums as indicated in Figure 8 leaves the large HOMO–LUMO gap nearly unchanged. The b_{2g} and $1b_{3u}$ levels, on the other hand, drop sharply in energy to open a second gap, below $2a_g$. b_{2g} and $1b_{3u}$ are σ bonding between the paired molybdenums and contribute substantially to the strong apical Mo–Mo bonding. The totally bonding levels $1a_g$ and b_{1u} remain nearly unchanged in energy throughout the deformation. Total energy follows the trend shown in Figure 8 and drops all along the distortion coordinate.

The small HOMO–LUMO gap and the gap between $1b_{3u}$ and $2a_g$ raise the natural question whether or not $Mo_{22}O_{34}^{8-}$ could be oxidized or reduced. The answer is, most probably, yes. $Mo_{18}O_{28}^{7-}$ might provide one extra electron since its HOMO is at nearly the same energy, but slightly above, $2b_{3u}$ in Figure 8. Transferring a single electron from $Mo_{18}O_{28}^{7-}$ would also leave it with a large HOMO–LUMO gap of nearly 0.5 eV. This combination of occurrences—(1) the HOMO of $Mo_{18}O_{28}^{7-}$ higher than the LUMO for $Mo_{22}O_{34}^{8-}$, (2) the large gap below the HOMO for $Mo_{18}O_{28}^{7-}$, and (3) the equally substantial energy gap between $2b_{3u}$ and the next highest level of $Mo_{22}O_{34}^{8-}$—all point to formulating $Mo_{40}O_{62}^{15-}$ as $Mo_{18}O_{28}^{6-}$ plus $Mo_{22}O_{34}^{9-}$. This new electron count gives a similar energy lowering for the distorted $Mo_{22}O_{34}^{9-}$ cluster, since the new HOMO stays at nearly constant energy during the pairing distortion.

Table I. Preferred Distortions for $Mo_{18}O_{28}^{n-}$ and $Mo_{22}O_{34}^{n-}$ for Different Electron Counts

molecule/charge	distortion
$Mo_{18}O_{28}^{n-}$	
$n = 7$	pairing
$n = 6$	pairing
$n = 4$	tilting
$Mo_{22}O_{34}^{n-}$	
$n = 9$	tilting/pairing
$n = 8$	tilting/pairing
$n = 6$	tilting

Could the "extra" electron occupy an In-based orbital, instead of being located on the molybdate clusters? We think not. Treating the In chains as separate subsystems puts the LUMO for In_6^{8+} at −8.1 eV, more than 2 eV above the HOMO of either $Mo_{18}O_{28}^{6-}$ or $Mo_{22}O_{34}^{9-}$. Thus the unoccupied indium orbitals will mix very little with occupied molybdate levels, and the indium chains are best described as before, as In_5^{7+} and In_6^{8+}.

An alternative octahedral tilting was also considered and found to give an energy lowering identical with that for the pairing distortion. The reason is a simple one. In the Mo_{18} cluster, the orbitals with one node perpendicular to the chain mixed upon distortion to give a bonding and an antibonding level. The antibonding level had a substantial amplitude on two neighboring molybdenums and opposed the tilting deformation. The corresponding orbitals for $Mo_{22}O_{34}^{8-}$ are noded on apical molybdenums at the center of the molecule. Neighboring Mo atoms for $Mo_{22}O_{34}^{8-}$, or for any such cluster formed from an odd number of trans-edge-sharing octahedra, can never build up the antibonding interaction illustrated for the Mo_{18} cluster in **18**. A group theoretical explanation is equally simple: octahedral tilting reduces the symmetry of $Mo_{18}O_{28}^{7-}$ to C_{2v}, but $Mo_{22}O_{34}^{8-}$ becomes C_{2h}.

Table II. Parameters Used in the Extended-Hückel Calculations

orbital		H_{ii} (eV)	ζ_1 (C_1[a])	ζ_2 (C_2[a])
Mo	4d	-11.06	4.54 (0.5899)	1.90 (0.5899)
	5s	-8.77	1.96	
	5p	-5.60	1.90	
In	5s	-12.60	1.903	
	5p	-6.19	1.677	
O	2s	-32.3	2.275	
	2p	-14.8	2.275	
H	1s	-13.6	1.40	

[a] Coefficients in the double-ζ d orbital expansion.

The relevant levels of $Mo_{22}O_{34}^{8-}$, labeled b_{2g} and $1b_{3u}$ in Figure 8, become b_g and b_u in the distorted structure and cannot mix. In fact, both levels drop in energy with octahedral tilting. The bonding situation for Mo pairing or octahedral tilting in $Mo_{22}O_{34}^{8-}$ is succinctly summarized in **20**. **20** shows that pairing and tilting each form four strong Mo–Mo bonds between apical molybdenums.

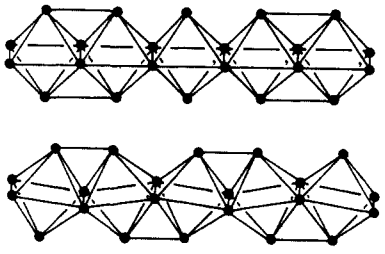

20

Conclusions

Mo–Mo bonding in $Mo_{18}O_{28}^{7-}$ was analyzed in detail, in terms of parallel metal chains at the apex or in the basal planes of the component octahedra. The experimentally observed variation in Mo–Mo bond lengths parallel to the chain was attributed to the occupation of x^2-y^2 levels of C_{2v} ML_4 (basal molybdenums) and C_{4v} ML_5 (apical Mo) fragments. The basal x^2-y^2 levels are low in energy and filled through the level with one node perpendicular to the chain, similar to the π system of butadiene. Like the carbon atoms in butadiene, basal molybdenums in $Mo_{18}O_{28}^{7-}$ pair up at the ends of the chain.

Apical Mo x^2-y^2 orbitals appear near the HOMO–LUMO gap and suggest several interesting distortions to form apical Mo–Mo bonds, depending on the d electron count at the metal. The energy gap that opens up below the singly occupied $5a_g$ orbital in $Mo_{18}O_{28}^{7-}$, as well as a LUMO for $Mo_{22}O_{34}^{8-}$ that appears slightly below $5a_g$, suggests that the experimentally observed clusters may be better formulated as $Mo_{18}O_{28}^{6-}$ and $Mo_{22}O_{34}^{9-}$. It will be difficult to test this prediction experimentally since singly occupied orbitals on $Mo_{18}O_{28}^{7-}$ or $Mo_{22}O_{34}^{9-}$ both have b_{3u} symmetry and differ only in the extent of delocalization along the chain.

Several possible distortions exist for the $Mo_{22}O_{34}^{8-}$ cluster as well, depending on electron count. Predicted distortions—a simple pairing of apical molybdenums or a tilting of octahedra—are summarized for both molecules, for a variety of different electron counts, in Table I.

$Mo_{18}O_{28}^{n-}$ shows a definite preference for the pairing or for the tilting distortion, whereas $Mo_{22}O_{34}^{n-}$ often finds Mo pairing or octahedron tilting equally favorable. The preference of $Mo_{18}O_{28}^{6-,7-}$ for pairing was traced to orbital topology. For a chain such as $Mo_{18}O_{28}$—with an even number, N, of octahedra—pairing apical molybdenums forms N metal–metal bonds, but tilting of octahedra can only form $N-1$ bonds. For odd N, both pairing and tilting form the same number of strong Mo–Mo bonds and are equally favorable. The energy difference between pairing and tilting can be removed for even N by emptying one bonding level. In $Mo_{18}O_{28}^{6-}$ the orbital that is emptied on going to $Mo_{18}O_{28}^{4-}$ is the singly noded $1b_{2g}$ level. The difference between even- and odd-member chains is an "end effect" that decreases as N increases, as the chain grows longer.

The pairing of apical molybdenums along the chain and basal Mo–Mo bonding perpendicular to the chain are electronically coupled. An empty level with a substantial contribution from basal molybdenums at the ends of the chain mixes with occupied levels when apical molybdenums pair. The mixing strengthens primarily those basal Mo–Mo bonds (perpendicular to the chain) that are located at the chain ends.

Acknowledgment. We thank Susan A. Jansen and Jing Li for helpful discussions and the Cornell University Materials Science Center for funding through Grant No. DMR 87422702 from the NSF.

Appendix

Extended-Hückel calculations[23] were carried out with use of the parameters listed in Table II. Molybdenum[21a] and indium[29] exponents and Coulomb integrals were taken from previous publications. Cluster geometries were idealized, with Mo–Mo distances of 2.80 Å along the chain axis and 2.75 Å between apical and basal molybdenums; Mo–O distances were taken as 2.00 Å.

The $C_4H_7^+$ Cation. A Theoretical Investigation

Wolfram Koch,*[†] Bowen Liu,[†] and Douglas J. DeFrees[‡]

Contribution from IBM Almaden Research Center, 650 Harry Road, San Jose, California 95120-6099, and Molecular Research Institute, 701 Welch Road, Palo Alto, California 94304. *Received March 10, 1988*

Abstract: The potential energy surface of the $C_4H_7^+$ cation has been investigated with ab initio quantum chemical theory. Extended basis set calculations, including electronic correlation, show that cyclobutyl and cyclopropylcarbinyl cation are equally stable isomers. The saddle point connecting these isomers lies 0.6 kcal/mol above the minima. The global $C_4H_7^+$ minimum corresponds to the 1-methylallyl cation, which is 9.0 kcal/mol more stable than the cyclobutyl and the cyclopropylcarbinyl cation and 9.5 kcal/mol below the 2-methylallyl cation. These results are in excellent agreement with experimental data.

The structures, reactions, and energetics of the $C_4H_7^+$ cation have received continued attention ever since the discovery of facile interconversion of cyclopropylcarbinyl, cyclobutyl, and allylcarbinyl derivatives in aprotic solvents by Roberts, more than 35 years ago.[1-4] In solution, it is now firmly established that $C_4H_7^+$ generated from cyclopropylcarbinyl or cyclobutyl derivatives has more than one structure. Available experimental information can

[†] IBM Almaden Research Center.
[‡] Molecular Research Institute.

(1) Richey, G. In *Carbonium Ions*; Olah, G. A., Schleyer, P. v. R., Eds.; Wiley Interscience: New York, 1972; Vol III, Chapter 25.
(2) Wiberg, K. B.; Hess, B. A.; Ashe, A. J. In *Carbonium Ions*; Olah, G. A., Schleyer, P. v. R., Eds.; Wiley Interscience: New York, 1972; Vol. III, Chapter 26.

0002-7863/88/1510-7325$01.50/0